

MWIRSTD: A MWIR SMALL TARGET DETECTION DATASET

Nikhil Kumar^{†*} Avinash Upadhyay^{†*} Shreya Sharma^{‡§} Manoj Sharma[‡] Pravendra Singh[†]

[†] IIT Roorkee, [‡]Bennett University, [§]Visual Cognitive Laboratory Pvt Ltd,
[†] nikhil_k1@cs.iitr.ac.in, [‡] avinres@gmail.com, [‡] manoj.sharma1@bennett.edu.in,
[‡] e21cseu0601@bennett.edu.in, [†]pravendra.singh@cs.iitr.ac.in

ABSTRACT

This paper presents a novel mid-wave infrared (MWIR) small target detection dataset (MWIRSTD) comprising 14 video sequences containing approximately 1053 images with annotated targets of three distinct classes of small objects. Captured using cooled MWIR imagers, the dataset offers a unique opportunity for researchers to develop and evaluate state-of-the-art methods for small object detection in realistic MWIR scenes. Unlike existing datasets, which primarily consist of uncooled thermal images or synthetic data with targets superimposed onto the background or vice versa, MWIRSTD provides authentic MWIR data with diverse targets and environments. Extensive experiments on various traditional methods and deep learning-based techniques for small target detection are performed on the proposed dataset, providing valuable insights into their efficacy. The dataset and code are available at <https://github.com/avinres/MWIRSTD>.

Index Terms— Small target detection, small and dim target detection, point target detection, MWIR, dataset, defence application

1. INTRODUCTION

The electromagnetic spectrum’s infrared (IR) band encompasses wavelengths from 700 nm to 1 mm. Table 1 outlines the various bands within the IR spectrum commonly used for imaging applications. It’s worth noting that while the IR spectrum shares its lower end with the visible spectrum’s red edge, research suggests that a considerable portion of the IR spectrum is unsuitable for typical imaging due to poor transmission characteristics [1, 2].

In both military and civilian realms, the precise detection of small objects in IR imaging holds significant importance. Modern computer vision algorithms leverage deep neural networks and data-driven machine learning techniques to achieve this. These algorithms aim to enhance object detection accuracy while minimizing false alarms. However, the efficacy of such approaches heavily relies on robust datasets for training and validation [3]. Despite the growing demand for

Table 1. Various bands in IR spectrum for imaging.

Band	Wavelength
Near Infrared (NIR)	0.7um-0.9um
Short Wave Infrared (SWIR)	0.9um-2.5um
Mid Wave Infrared (MWIR)	3um-5um
Long Wave Infrared (LWIR)	8um-12um

high-quality datasets, publicly available resources often fall short. Many existing datasets are constructed by overlaying pre-recorded IR image backgrounds with superimposed targets. This approach, while helpful, lacks the authenticity and complexity of real-world scenarios. Addressing this gap, our study utilized a cooled mid-wave infrared (MWIR) imager to capture video sequences featuring small targets in authentic environments. This endeavour resulted in the creation of the first publicly available dataset focused on small targets captured in MWIR. This dataset represents a valuable asset for developing algorithms tailored to defence applications. Furthermore, a noteworthy characteristic of the dataset is that many small targets exhibit spatio-temporal regularity during motion. This inherent feature makes the dataset suitable for object detection and well-suited for tracking purposes.

1.1. Significance of small targets in MWIR imagery

Due to the high temperatures, military targets like missiles and aircraft plumes exhibit more prominent signatures in the Medium-wave infrared (MWIR) band than in the long-wave infrared (LWIR) band. The MWIR band plays a critical role in IR countermeasure activities. Several electro-optical systems used in aerial countermeasure activities, such as IR Search and Track (IRST) and Missile Approach Warning Systems (MAWS), are designed to operate within this specific range of the electromagnetic spectrum, as discussed in works [10] and [11]. These systems detect potential threats over long distances, sometimes spanning hundreds of kilometres. Targets of military importance are typically large and emit strong infrared radiation. However, they often appear small and faint in images due to their small angular projection on the imaging plane and significant transmission losses. These

*Equal Contribution

Table 2. Details of various available datasets commonly used in small target detection. Table courtesy [4].

Dataset	Image Type	Background Scene	Number of Images	Label Type	Target Type	Availability
NAAA-SIRST [5]	Real	Cloud/City/Sea	427	Manual Coarse Label	Point/Spot/Extended	Public
NUST-SIRST [6]	Synthetic	Cloud/City/River/Road	10,000	Manual Coarse Label	Point Spot	Public
CQU-SIRST [7]	Synthetic	Cloud/City/Sea	1676	Ground Truth	Point Spot	Private
NUDT-SIRST [8]	Synthetic	Cloud/City/Sea/Highlight/Field	1327	Ground Truth	Point/Spot/Extended	Public
IRSTD [9]	Real	Sea/River/Field/Mountain/City/Cloud	1000	Ground Truth	Point/Spot/Extended	Public

losses, which involve absorption and scattering [3], become increasingly noticeable when travelling long distances. Occasionally, when dealing with long distances, the signatures of certain targets may be limited to just one or two pixels. Even at closer distances, the target can continue to appear small in the image plane. Unfortunately, it will be a complex task to simultaneously fly multiple aircraft and missiles in order to generate datasets for the purpose of detecting and tracking small targets. Small targets usually only cover a small portion of the pixels, leading to a scarcity of spatial features. The infrared signatures can vary over time with the changing thermodynamics of the scene and the shifting visual aspect angle of the seen object relative to the position of the imaging device. Infrared imaging frequently experiences significant amounts of noise and background clutter, which may obscure targets, decrease contrast, and lead to a reduced Signal-to-Clutter Ratio (SCR). IR small targets have a lower contrast ratio than small targets in RGB images, resulting in a more considerable similarity to the background. This similarity makes it more difficult to differentiate such targets from their surroundings. Applying well-known deep learning object detection algorithms such as the RCNN series [12], YOLO series [13], and SSD [14] for detecting small and dim point targets is not ideal. This is because the pooling layers in these networks may cause the loss of these targets in deeper layers. Researchers have dedicated their efforts to creating specialized deep networks that can effectively identify small infrared targets.

2. RELATED WORK

The proposed work presents a novel Mid-Wave Infrared (MWIR) dataset specifically tailored for small target detection. This section reviews existing datasets relevant to small target detection and provides a comparative analysis of their characteristics.

Several existing datasets play a crucial role in advancing small target detection methodologies. Notable among them are NAAA-SIRST Dataset [5], NUST-SIRST Dataset

[6], CQU-SIRST Dataset [7], NUDT-SIRST Dataset [8] and IRSTD Dataset [9]. Each of these datasets offers unique challenges and scenarios for algorithm assessment. Table 2 provides a detailed comparison, highlighting key attributes such as dataset size, diversity, and scene complexity across datasets. One of the main limitations of these datasets is that they do not claim to be captured in MWIR. Additionally, many of them have used a target overlay approach on a recorded background, which means they are not representative of real scenarios. On the other hand, this work presents a real dataset captured through a cooled MWIR imager. While these datasets contribute significantly to the field, there remains a need for a specialized real dataset that focuses specifically on the real challenges associated with small target detection within the MWIR spectrum.

In addition to existing datasets, researchers have developed their own distinct datasets to evaluate the performance of their algorithms. Liu et al. [15] conducted a study involving the creation of a dataset [16] aimed at assessing their algorithm's capabilities. Similarly, Kumar et al. [17] developed a dataset tailored to their specific research objectives. These custom datasets enable researchers to tailor scenarios to their algorithm's strengths and weaknesses, providing a more targeted evaluation.

A noteworthy methodology introduced by Naraniya et al. (2021) involves the creation of a specialized dataset through the combination of artificially generated backgrounds with synthetic targets. In this approach, the movement of the target is represented in the NED coordinate system, and Gaussian blurred small targets are superimposed onto backgrounds. This unique dataset creation method adds variability and complexity to the dataset, closely simulating real-world scenarios. While existing small target detection datasets have significantly contributed to advancing target detection algorithms, the proposed work introduces a novel dataset specifically designed for small target detection in MWIR images.

Table 3. Details of Imager used for dataset generation.

Parameter	Specification	Remark
Spectral range	$3\mu\text{m} - 5\mu\text{m}$	MWIR
Type	Cooled	Stirling cycle
FPA resolution	640 X 512	InSb
FOV (widest)	$12^\circ \times 9^\circ$	Continuous Zoom
FOV(narrow)	$0.9^\circ \times 0.7^\circ$	

3. PROPOSED DATASET

3.1. Data Collection

A MWIR imager, with the specifications outlined in Table 3, was installed on a mountain where the environmental conditions described in Table 4 were present. Throughout the exercise, the slant distance between the object and the imager ranged from 300 meters to 950 meters, with the imager mostly in the wide field of view (WFOV).

3.2. Pre processing

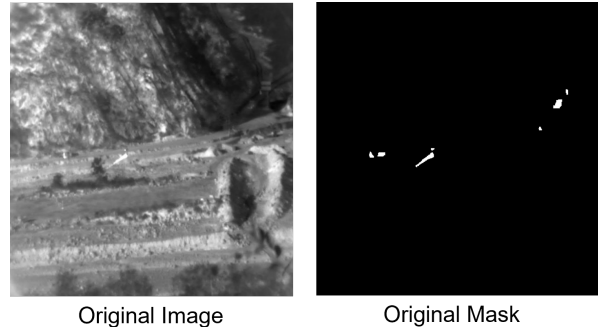
The imager transmits out the live video in PAL-B format at a frame rate of 25 frames per second. Because of the analog nature of the video output, a frame grabber card was used to convert and record this information in a digital format. Even though it produces a monochrome video sequence, the images are saved as '.jpg' files with three channels due to the frame grabber hardware settings. During the pre-processing stage, the authors extracted sequences with pertinent information from a lengthy video sequence. The dimensions of all extracted frames were resized to 509×655 to exclude areas that do not contain useful information.

3.3. The Ground truth

Given that the goal of this setup was to capture small objects in the MWIR range, the authors utilized cracker rockets. In certain situations, a road serves as the background, while multiple moving automobiles function as small targets. The ground truth data includes labels for moving ground vehicles. As shown in Figure 1 and Figure 2, there are three types of labels that are annotated in the ground truth. The first class of annotation has been accomplished for cracker rockets, while the second class of annotation pertains to the debris resulting from these rockets. The third class of annotation is reserved for other moving targets in the scenario, which are often categorized as small targets. Table 5 provides a detailed description of the content found in all 14 recorded sequences of the dataset.

Table 4. Environmental parameters during dataset collection.

Parameter	Value
Wind Speed	6 mph
Humidity	72 %
Temperature	$11.6^\circ\text{C} - 15^\circ\text{C}$
Time	1400-1700 hrs GMT+0530
Visibility	Poor (Hazy environment)

**Fig. 1.** A typical frame of the proposed dataset and its mask.

4. EXPERIMENTS

4.1. Evaluation Metric

The proposed dataset was evaluated using two widely used metrics, i.e., IoU (Intersection over Union) and PD (Probability of Detection) at the pixel level, to assess the effectiveness of different image processing based computation and deep learning methods. Further, the FAR (False alarm Rate) at the pixel level was also used to provide a more detailed analysis of the results. We have selected these metrics as they are commonly used in target segmentation scenarios and provide a balanced measure of both detection accuracy and precision. Specifically, IoU evaluates the overlap between the predicted bounding box and the ground truth, while PD assesses the ratio of correctly detected pixels as the target to the total number of pixels detected as a target. Furthermore, calculating FAR helps identify any potential issues with false positives, which can be critical in applications where accurate detection is crucial.

4.2. Results and Analysis

In this section, we present the evaluation results of six traditional small object detection methods: Top-hat Morphology (TPHT) [18], Modified Top Hat Morphology (MTHM) [19, 20], Maxmean [21], MLCM [22], MRCM [23], and DGRAD [24] and two state-of-the-art deep learning-based methods U-Net [25], DNA-Net [8] on our proposed MWIR dataset. We employed two commonly used metrics, i.e., mean Intersection

Table 5. Details of the proposed dataset including sequence number, number of frames, frame size, target details, background composition, and other relevant information.

Seq No	Number of Frames	Frame Size	Target Details	Background Composition	Additional Information
1	78	509x655 (8-bit)	Single Cracker rocket with its debris	Open Field/Road/Mountain/Vegetation/Houses	Target motion across less, cluttered vegetation and open field
2	73	509x655 (8-bit)	Single Cracker rocket with its debris	Open Field/Road/Mountain/Vegetation/Houses	
3	63	509x655 (8-bit)	Single Cracker rocket with its debris	Open Field/Road/Mountain/Vegetation/Houses	The target motion also encompasses a densely cluttered region. Almost vertical path. Almost complete FOV is covered by the target.
4	65	509x655 (8-bit)	Single Cracker rocket with its debris	Open Field/Road/Mountain/Vegetation/Houses	The target trajectory covers both open field as well as densely cluttered region. Almost vertical path.
5	119	509x655 (8-bit)	Single Cracker rocket with its debris	Open Field/Road/Mountain/Vegetation/Houses	Target motion across less cluttered vegetation and the open field
6	93	509x655 (8-bit)	Single Cracker rocket with its debris	Open Field/Road/Mountain/Vegetation/Houses	
7	74	509x655 (8-bit)	Single Cracker rocket with its debris, Multiple moving Vehicles as small targets	Open Field/Road/Mountain/Vegetation/Houses	Target motion across deep cluttered vegetation.
8	56	509x655 (8-bit)	Single Cracker rocket with its debris, Multiple moving Vehicles as small targets	Open Field/Road/Mountain/Vegetation/Houses	
9	83	509x655 (8-bit)	Single Cracker rocket with its debris, Multiple moving Vehicles as small targets	Open Field/Road/Mountain/Vegetation/Houses	
10	86	509x655 (8-bit)	Single Cracker rocket with its debris, Multiple moving Vehicles as small targets	Open Field/Road/Mountain/Vegetation/Houses	Parabolic trajectory
11	77	509x655 (8-bit)	Single Cracker rocket with its debris, Multiple moving Vehicles as small targets	Open Field/Road/Mountain/Vegetation/Houses	Almost Horizontal Trajectory
12	53	509x655 (8-bit)	Single Cracker rocket with its debris, Multiple moving Vehicles, pedestrians, two-wheeler inside FOV	Dense Forest / Road	Almost Horizontal Trajectory

Seq No	Number of Frames	Frame Size	Target Details	Background Composition	Additional Information
13	75	509x655 (8-bit)	Single Cracker rocket with its debris, Multiple moving Vehicles, pedestrians, two-wheeler inside FOV	Dense Forest / Road	
14	68	509x655 (8-bit)	Single Cracker rocket with its debris, Multiple moving Vehicles, pedestrians, two-wheeler inside FOV	Dense Forest / Road	Trajectory at 45 degrees

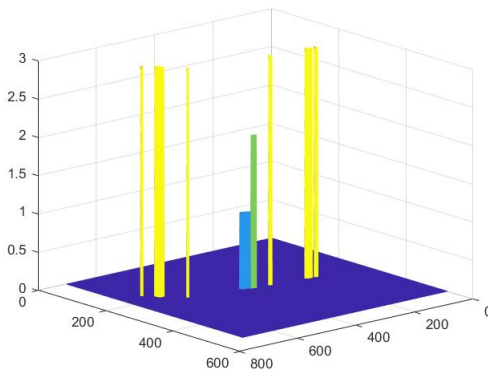


Fig. 2. The ground truth of the considered frame shown in Fig. 1 with annotations for three distinct classes. Class 1 refers to cracker rockets (shown in blue), Class 2 represents debris from cracker rockets (shown in green), and Class 3 includes other small moving targets (shown in yellow).

over Union (IoU) and mean Probability of Detection (PD), to evaluate the performance of these methods. Additionally, we calculated the mean False Alarm Rate (FAR) at the pixel level to analyze the results further. The deep-learning-based models were trained from scratch on our datasets. Initially, IoU, Pd, and FAR are calculated on a frame basis, and then their mean value for the complete test set has been presented here. TPHT is based on conventional top hat morphological operation. In this case, a 5×5 square structuring element has been taken. MTHM is a modified version of classical top hat morphology, and in this, a ring-type structuring element has been considered in place of the square structuring element in the previous case. Maxmean is a statistical algorithm, and while implementing this, the Maxmean operation is implemented on 5×5 window of the image. MLCM, MRCM, and DGRAD use image contrast as a primary feature and define some handcrafted feature extraction operations; based on these operations, any particular pixel is declared as part of the foreground or background. One of the standard requirements

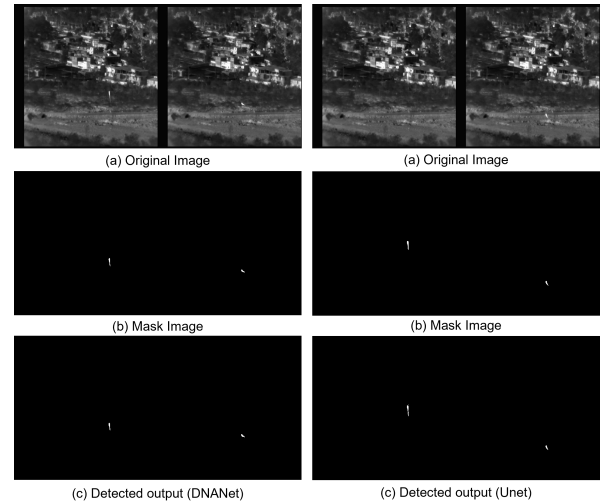


Fig. 3. Visual results obtained using Deep learning-based methods.

for all of the above approaches is the segmentation of the detection plane, and for this activity, the following threshold has been chosen as

$$Threshold = Imagemean + 0.5 * (Imagemax - Imagemean)$$

As observed from Table 6, all the traditional methods exhibit suboptimal performance on our dataset. In contrast, the deep learning-based methods demonstrated exceptional performance, with the U-Net method attaining an average IoU of 0.79 and PD of 0.1124. These findings indicate that deep learning techniques surpass traditional computational approaches in detecting small objects in MWIR images.

Table 6 demonstrates the ability of the deep learning-based methods to accurately detect and segment small objects in MWIR images, while the traditional computational methods often produce fragmented or incomplete detections. Overall, our results suggest that deep learning-based methods are superior to traditional computational approaches for small object detection in MWIR imagery. Fig. 3, Fig. 4, and

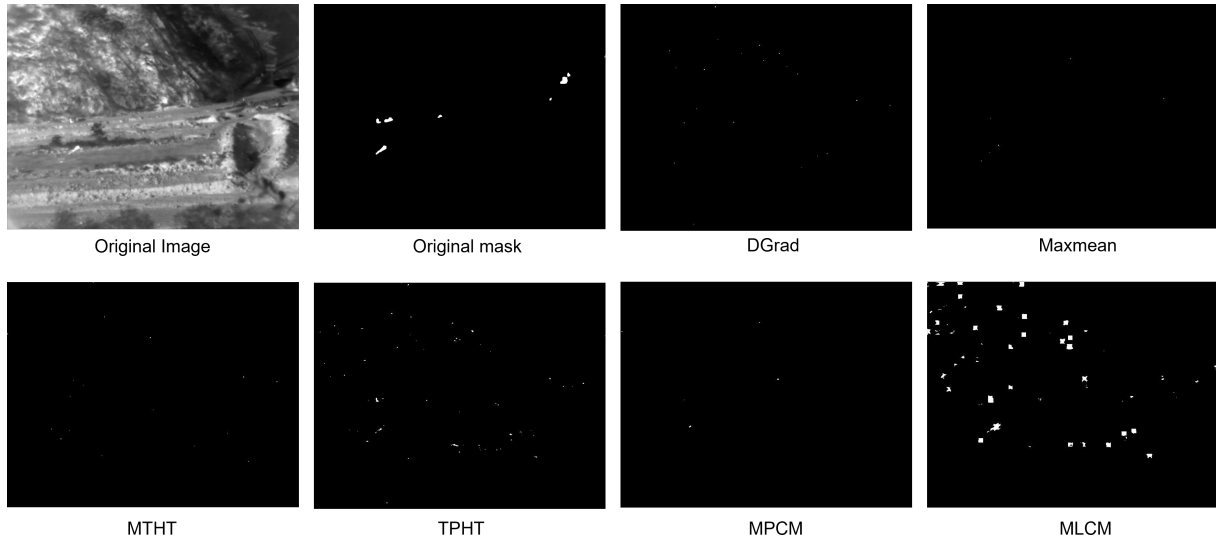


Fig. 4. Visual results obtained using traditional computational methods.

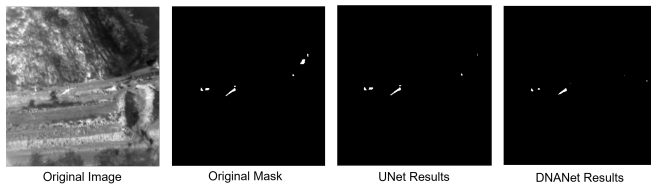


Fig. 5. Failed cases for Deep learning-based models.

Fig. 5 present a glimpse of visual results obtained using the proposed dataset.

5. CONCLUSION

This dataset, the first ever to capture MWIR with real small targets and real backgrounds, will provide a strong foundation for researchers in this field. Currently, the dataset comprises 14 sequences with a diverse range of foreground and background combinations, making it an ideal testbed for training and validating advanced deep-learning models for detecting small and dim targets. A benchmarking study has revealed that techniques employing deep learning models demonstrate exceptional performance, exhibiting a higher probability of detection while maintaining a lower false alarm rate. The targets in these sequences exhibit a consistent spatiotemporal regularity pattern, suggesting potential for future expansion of this dataset to address tracking-related challenges.

6. REFERENCES

[1] Gerald C Holst, *Common sense approach to thermal imaging*, vol. 1, SPIE Optical Engineering Press Washington, 2000.

Table 6. Performance benchmark evaluation using several traditional and deep learning-based approaches over the proposed dataset.

Algorithm	IoU	POD	FAR
Maxmean	0.0036	0.018	0.9931
THM	0.002	0.024	0.997
MTHM	0.0037	0.0164	0.992
MLCM	0.0027	0.046	0.996
MPCM	0.0033	0.007	0.9858
DGRAD	0.0031	0.007	0.9829
U-NET	0.7945	0.8855	0.1124
DNA-NET	0.6440	0.7330	0.1569

[2] J Michael Lloyd, *Thermal imaging systems*, Springer Science & Business Media, 2013.

[3] Richard D Hudson, *Infrared system engineering*, vol. 1, Wiley-Interscience New York, 1969.

[4] Nikhil Kumar and Pravendra Singh, “Small and dim target detection in ir imagery: A review,” *arXiv preprint arXiv:2311.16346*, 2023.

[5] Yimian Dai, Yiquan Wu, Fei Zhou, and Kobus Barnard, “Asymmetric contextual modulation for infrared small target detection,” in *Proceedings of the IEEE/CVF Winter Conference on Applications of Computer Vision*, 2021, pp. 950–959.

[6] Huan Wang, Luping Zhou, and Lei Wang, “Miss detection vs. false alarm: Adversarial learning for small object segmentation in infrared images,” in *Proceedings of*

the *IEEE/CVF International Conference on Computer Vision*, 2019, pp. 8509–8518.

- [7] Chenqiang Gao, Deyu Meng, Yi Yang, Yongtao Wang, Xiaofang Zhou, and Alexander G Hauptmann, “Infrared patch-image model for small target detection in a single image,” *IEEE transactions on image processing*, vol. 22, no. 12, pp. 4996–5009, 2013.
- [8] Boyang Li, Chao Xiao, Longguang Wang, Yingqian Wang, Zaiping Lin, Miao Li, Wei An, and Yulan Guo, “Dense nested attention network for infrared small target detection,” *IEEE Transactions on Image Processing*, vol. 32, pp. 1745–1758, 2022.
- [9] Mingjin Zhang, Rui Zhang, Yuxiang Yang, Haichen Bai, Jing Zhang, and Jie Guo, “Isnet: Shape matters for infrared small target detection,” in *Proceedings of the IEEE/CVF Conference on Computer Vision and Pattern Recognition*, 2022, pp. 877–886.
- [10] Arie N de Jong, “Irst and its perspective,” in *Infrared Technology XXI*. SPIE, 1995, vol. 2552, pp. 206–213.
- [11] Hannes Holm Ovrén and Erika Emilsson, “Missile approach warning using multi-spectral imagery,” 2010.
- [12] Ross Girshick, Jeff Donahue, Trevor Darrell, and Jitendra Malik, “Rich feature hierarchies for accurate object detection and semantic segmentation,” in *Proceedings of the IEEE conference on computer vision and pattern recognition*, 2014, pp. 580–587.
- [13] Joseph Redmon, Santosh Divvala, Ross Girshick, and Ali Farhadi, “You only look once: Unified, real-time object detection,” in *Proceedings of the IEEE conference on computer vision and pattern recognition*, 2016, pp. 779–788.
- [14] Wei Liu, Dragomir Anguelov, Dumitru Erhan, Christian Szegedy, Scott Reed, Cheng-Yang Fu, and Alexander C Berg, “Ssd: Single shot multibox detector,” in *Computer Vision–ECCV 2016: 14th European Conference, Amsterdam, The Netherlands, October 11–14, 2016, Proceedings, Part I 14*. Springer, 2016, pp. 21–37.
- [15] Ming Liu, Hao-yuan Du, Yue-jin Zhao, Li-quan Dong, Mei Hui, and SX Wang, “Image small target detection based on deep learning with snr controlled sample generation,” *Current Trends in Computer Science and Mechanical Automation*, vol. 1, pp. 211–220, 2017.
- [16] Nikhil Kumar, Unnikrishnan Gopinathan, Neeta Kandpal, and Ajay Kumar, “Point target detection for maws application,” in *2023 3rd International Conference on Range Technology (ICORT)*, 2023, pp. 1–6.
- [17] Nikhil Kumar, Sandeep Kumar, Zahir A Ansari, Neeta Kandpal, G Unnikrishnan, and Ajay Kumar, “Detection of point targets amid cluttered background in ir imagery for irst and maws applications,” in *2021 2nd International Conference on Range Technology (ICORT)*. IEEE, 2021, pp. 1–6.
- [18] Rafael C Gonzalez, Richard Eugene Woods, and Steven L Eddins, *Digital image processing using MATLAB*, Pearson Education India, 2004.
- [19] Xiangzhi Bai, Fugen Zhou, and Yongchun Xie, “New class of top-hat transformation to enhance infrared small targets,” *Journal of Electronic Imaging*, vol. 17, no. 3, pp. 030501–030501, 2008.
- [20] Xiangzhi Bai, Fugen Zhou, and Ting Jin, “Enhancement of dim small target through modified top-hat transformation under the condition of heavy clutter,” *Signal Processing*, vol. 90, no. 5, pp. 1643–1654, 2010.
- [21] Yanfeng Gu, Chen Wang, Baoxue Liu, and Ye Zhang, “A kernel-based nonparametric regression method for clutter removal in infrared small-target detection applications,” *IEEE Geoscience and Remote Sensing Letters*, vol. 7, no. 3, pp. 469–473, 2010.
- [22] C. L. Philip Chen, Hong Li, Yantao Wei, Tian Xia, and Yuan Yan Tang, “A local contrast method for small infrared target detection,” *IEEE Transactions on Geoscience and Remote Sensing*, vol. 52, no. 1, pp. 574–581, 2014.
- [23] Yantao Wei, Xinge You, and Hong Li, “Multiscale patch-based contrast measure for small infrared target detection,” *Pattern Recognition*, vol. 58, pp. 216–226, 2016.
- [24] Lang Wu, Yong Ma, Fan Fan, Minghui Wu, and Jun Huang, “A double-neighborhood gradient method for infrared small target detection,” *IEEE Geoscience and Remote Sensing Letters*, vol. 18, no. 8, pp. 1476–1480, 2020.
- [25] Olaf Ronneberger, Philipp Fischer, and Thomas Brox, “U-net: Convolutional networks for biomedical image segmentation,” in *Medical Image Computing and Computer-Assisted Intervention–MICCAI 2015: 18th International Conference, Munich, Germany, October 5–9, 2015, Proceedings, Part III 18*. Springer, 2015, pp. 234–241.